Gene Expression Profiles Associated with Inflammation, Fibrosis, and Cholestasis in Mouse Liver after Griseofulvin

Timothy W. Gant,[1] Petra R. Baus,[1] Bruce Clothier,[1] Joan Riley,[1] Reginald Davies,[1] David J. Judah,[1] Richard E. Edwards,[1] Elisabeth George,[2] Peter Greaves,[1] and Andrew G. Smith[1]

[1]MRC Toxicology Unit, University of Leicester, Leicester, United Kingdom; [2]GlaxoSmithKline, Ware, Hertfordshire, United Kingdom

Erythropoietic protoporphyria patients can develop cholestasis, severe hepatic damage, fibrosis, and cirrhosis. We modeled this hepatic pathology in C57BL/6J and BALB/c mice using griseofulvin and analyzed 3,127 genes for alteration of expression in the liver before and during the onset of protoporphyria, cholestasis, inflammation, and hepatic fibrosis. The two mouse strains developed different levels of pathologic damage in response to the griseofulvin. Characteristic gene expression profiles could be associated with griseofulvin-induced gene expression, disruption of lipid metabolism, and the pathologic states of inflammation, early fibrosis, and cholestasis. Additionally, some genes individually indicated an alteration of homeostasis or pathologic state; for example, fibroblast proliferation was potentially indicated by increased calcyclin (SA100a6) expression. Changes in cytochrome P450 (*Cyp*) gene expression were particularly pronounced, with increased expression of the *Cyp2a, Cyp2b,* and *Cyp3a* families. Decreased *Cyp4a10* and *Cyp4a14* expression was observed that could be associated with early pathologic change. A potential decrease in bile acid and steroid biosynthesis was indicated by the decreased expression of *Cyp7b1* and *Hsd3b4,* respectively. DNA damage was indicated by induction of *GADD45*. This study illustrates how transcriptional programs can be associated with different stimuli in the same experiment. The time course of change in the gene expression profile compared with changes in pathology and clinical chemistry shows the potential of this approach for modeling causative, predictive, and adaptive changes in gene expression during pathologic change. *Key words:* fibrosis, inflammation, liver, microarray, protoporphyria. *Environ Health Perspect* 111:847–853 (2003). doi:10.1289/txg.5849 available via *http://dx.doi.org/* [Online 18 November 2002]

Chronic liver injury from diverse causes such as viruses, parasites, alcohol, hereditary metal overload, for example, Wilson disease, and xenobiotics may give rise to a constellation of abnormalities such as fatty change, apoptosis, necrosis, cholestasis, inflammation, and fibrosis as well as nodular regeneration and cirrhosis. As a paradigm for parenchymal wound healing in other tissues, chronic liver injury involves the activation of cytokines believed not only to mediate inflammation, necrosis, apoptosis, and fibrosis but also regeneration of liver tissue (Tilg and Diehl 2000). As with many diseases, progression reflects a combination of genetic and environmental factors, and the severity of the inflammatory process usually correlates with the rate of disease progression. In hereditary conditions such as hemachromatosis, a concurrent insult such as alcohol ingestion will increase injury and rate of progression to fibrosis (Friedman 1993). Other complicating factors include older age, immune status, male gender, and obesity (Friedman 1993; Tilg and Diehl 2000). Drug-induced liver injury also continues to be a significant problem (Bissell et al. 2001) where genetically determined differences in drug-metabolizing enzymes in the generation of toxic metabolites as well as in immune responses may be important (Lee 1995). However, the relative importance of these genetic factors and the way they might interact are not fully understood. One approach to help understand these factors and their interaction in the evolution of liver injury is through the use of gene expression profiles.

Griseofulvin is an antifungal agent that, when administered chronically to mice, produces a variety of hepatic responses the chronology of which have been extensively studied (Knasmuller et al. 1997). Early cell proliferation leads to an increase in liver/body weight ratio, and alteration of the liver drug-metabolizing profile (Knasmuller et al. 1997). One of the earliest features of griseofulvin exposure is a hepatic porphyria characterized by the accumulation of protoporphyrin IX (De Matteis and Rimington 1963; Weston Hurst and Paget 1963). This porphyria is induced by the inhibition of ferrochelatase probably caused by a griseofulvin adduct of protoporphyrin IX produced in a cytochrome P450 (*Cyp*)-mediated suicide reaction (Bellingham et al. 1995). The changes in liver pathology with griseofulvin are similar to those found with human erythropoietic protoporphyria (EP)-associated liver failure that occurs in a subset of patients and probably depends on genetic and physiologic susceptibility factors to determine its onset (Bloomer et al. 1998; Cox et al. 1998; Kappas et al. 1995).

Previous studies have used transcriptome data to categorize the toxicity of chemicals according to their gene expression profile, the premise being that those chemicals with a different type and/or mechanism of toxicity will produce different gene expression patterns. This approach was used by Waring et al. (2001) to distinguish 15 different hepatotoxins, a study which illustrated the utility of this approach. Similar studies have been carried out on smaller compound sets by Hamadeh et al. (2002a, 2002b). Working on the hypothesis that it is necessary using statistical analysis to determine only a relatively small number of gene expressions to differentiate toxicity profiles, Thomas et al. (2001) used 12 transcripts to differentiate a set of 12 hepatotoxins. This approach is potentially reductionist, however, and although successful on 12 previously characterized hepatotoxins, there is no guarantee that it works on novel agents using such a small number of genes. None of the above studies have addressed the potential influence of cellular response, altered organ homeostasis, and resulting pathologic change on gene expression profiles. This issue was addressed later by Hamadeh et al. (2002c), who were able to associate gene expression profiles with pathologic change in the liver after methapyrilene exposure. By making a correlation between gene expression profiles and pathologic change, these authors were able to demonstrate the ability of gene expression profile data to inform and enhance rather than replace the pathologic analysis. The application of gene expression profiles in toxicology and pathology has been recently reviewed (Gant 2002).

This article was previously published in the inaugural Toxicogenomics Section of *EHP*.

Address correspondence to T.W. Gant, MRC Toxicology Unit, Hodgkin Building, PO Box 138, University of Leicester, Leicester, LE1 9HN UK. Telephone: 44 116 252 5579. Fax: 44 116 252 5616. E-mail: twg1@le.ac.uk

We acknowledge the hard work of J. Edwards in the preparation of tissues sections, the staff of the biomedical services (University of Leicester), in particular, C. Travis. P. Baus was the recipient of a GlaxoSmithKline PLC studentship award.

Received 19 June 2002; accepted 18 November 2002.

In this study, cDNA microarray analysis was used to generate gene expression profiles associated with the early development of protoporphyria and the complex pattern of liver pathology that developed. These gene expression profiles then were used to produce a molecular map of pathologic change and griseofulvin exposure in this system.

Materials and Methods

Griseofulvin treatment of mice. Male BALB/c and C57BL/6J mice were obtained from Harlan Olac (Bicester, UK) at 6 weeks of age and acclimatized for 1 week on Rat and Mouse No. 1 maintenance (RMI; Special Diet Services, Witham, UK) fine ground diet prior to use. Animals were housed in negative pressure isolators at approximately 21°C with a 12-hr light-dark cycle. After acclimatization the diet was changed to one of RMI F.G. (fine ground) as above but containing either 2% arachis oil alone (control mice) or 2% arachis oil and 1% griseofulvin (w/w) obtained from Sigma Ltd. (Poole, Dorset, UK). Dose selection was based on prior experience and published data (De Matteis et al. 1966). Experiments were performed in accordance with Home Office license number 80/1329. Diet consumption was assessed by weighing the hoppers before refilling with diet on a daily basis, and indicated an approximately equal consumption by all groups. Animals were weighed every 3 days and removed from the study if the body weight fell below 80% of controls (one BALB/c animal was removed from the study on this basis). At the indicated times, blood was removed by cardiac puncture under halothane anesthesia before sacrifice by cervical dislocation. The liver was removed quickly for histology or stored in liquid nitrogen for RNA extraction.

Histologic methods. Liver tissue was fixed in 10% neutral buffered formalin and conventional histologic sections 5 μm thick were prepared and stained with hematoxylin and eosin and Van Gieson's stain for collagen. The study pathologist assessed the amount of hepatic pigment deposition and the degree of portal tract inflammation/bile duct proliferation in all animals in a blinded manner. A limited four-point scale was used to assure consistency (Shackelford et al. 2002). No lesion was represented by 0, minimal = 1, moderate = 2, and severe = 3. The scores were summated for each group of four mice to provide an overall estimate of the severity of these changes at each time point.

Clinical chemistry. Protoporphyria was assessed by estimation of the protoporphyrin content of the liver determined by spectrofluorimetry using the method of Grandchamp et al. (1980). Plasma aspartate aminotransferase (AST), alanine aminotransferase (ALT), and alkaline phosphatase (AP) were measured using kits from Sigma, according to the manufacturer's instructions.

Microarray analysis of gene expression. Analysis of gene expression was carried out using cDNA arrays containing 3127 EST (expressed sequence tag) clones for unique genes. There were quadruplicate sets of mice (control and treated) at each time point for each strain, and one array was used for each pair of mice. Thus, there were four sets of differential expression data for each time point in each strain. Microarray preparation, RNA labeling and hybridization were carried out as previously described (Turton et al. 2001) using ESTs derived from Research Genetics or from the IMAGE collections held at the MRC Human Gene Mapping Project (*http://www.hgmp.mrc.ac.uk*). The average length of the clones spotted on the array was 1028 bp. Fluorescent data derived from microarray features where either the polymerase chain reaction preparation of the clone had failed or a single product band had not been obtained were removed from the data set prior to normalization and analysis. The clone databases detailing the clones used on these arrays can be accessed from the MRC Toxicogenomics Unit website (*http://www.le.ac.uk/cmht/microarray_lab/Home*). The clones shown in the figures were sequenced to confirm identity.

Data analysis. Data analysis was carried out as previously described (Turton et al. 2001). Briefly, a measure of the median fluorescent intensity of the pixels within the hybridized feature area on the microarray for each gene was obtained using an Axon 4000A scanner (Axon Instruments, Inc. Union City, CA, USA). The measure of fluorescent feature intensity was accepted for further analysis if greater than 1.2 times the local background. The threshold above background was determined empirically as that required to avoid using measures of fluorescence in the low intensity range where variance between experimental replicates is high. Normalization of the channels was carried out using the median fluorescence feature intensity for each channel, as previously described (Turton et al. 2001), which was calculated after removal from the data set of all features where there was no polymerase chain reaction (PCR) product or the PCR product was not a single band on agarose gel analysis. The change in each gene expression was calculated by determining the fold change (ratio) of the normalized fluorescent intensities of each channel. These ratios were expressed on a $\log_2$ scale to normalize their distribution. Features where there were fluorescent data in one channel only were given an arbitrary $\log_2$ ratio value of 10 if the fluorescent intensity in the single channel was greater than 0.5 times the mean fluorescence intensity of the channel. For clustering purposes, changes in gene expression were assigned a score value on a scale or –1 to 1, depending on their position within the $\log_2$ (ratio) distribution, with those in the 95% confidence bands getting scores closer to 1 as previously described (Turton et al. 2001). Hierarchical clustering was then carried out using these score values. For the purposes of presentation, the $\log_2$ values were incorporated only in the clusters if the mean ratio change across the replicate experiments had a p value of <0.05 when compared with the population mean of the normalized data using a two-tailed t-test. This resulted in apparent anomalies in some time-course data points in Figure 3 where significance was not quite achieved due to high variance in the data at these particular points. These data points are shown as nondifferentially expressed, apparently contradicting the time-course trend. Software used in data analysis: for analysis of feature area fluorescent intensity, GenePix 3.0.0.85 or 3.0.5 (Axon Instruments); for data normalization, conversion, and statistical analysis, ConvertData 3.4.0c and Condenser 2.0.3 available from the MRC Toxicogenomics Unit website; for clone mapping and gene information updating, CloneMapper 1.0.4 (available on request from the corresponding author); for clustering and visualization, Cluster 3.0 and Treeview 1.5 (Eisen et al. 1998; *http://rana.lbl.gov*). Access2000 (Microsoft, Seattle, WA, USA) served the database requirements of this study. Interpretation of the data in terms of assigning function to the genes was achieved using information from the GeneCards (*http://nciarray.nci.nih.gov/cards*), GeneOntology from Amigo (*http://www.godatabase.org*) and GenomeNet (*http://www.genome.ad.jp*) databases in addition to literature searches.

Results

Histopathologic assessment of liver injury. Microscopic examination showed the pathologic change induced by griseofulvin was more apparent in C57BL/6J mice than in BALB/c mice (Figure 1). By day 1 only very minor focal inflammation in the C57BL/6J mice was seen, but more consistent focal inflammation was present by day 3 (Figure 1H). This was accompanied by deposition of red-brown pigment (protoporphyrin) from day 3 that was seen in the majority of the mice by day 5 (Figure 1G).

Thereafter, the amount of pigment in hepatocytes, bile ducts, and occasional Kupffer cells increased throughout the time course of the experiment but was usually greater in the C57BL/6J mice. Portal tract inflammation started to appear by day 5 consistently in the C57BL/6J mice in contrast to the BALB/c mice, where only one instance of a minor focal lesion was observed at this time point. The severity of inflammation and bile duct proliferation increased in the C57BL/6J mice throughout the time course of the study but again remained less marked in the BALB/c mice (Figure 1A–F). Focal parenchymal necrosis was also a feature of the treated C57BL/6J mice by days 5, 8, and 15 but was only seen to a minor extent in the BALB/c mice by day 22. Specific staining showed early fibrosis by day 15 in the livers of the C57BL/6J (Figure 1C) but not BALB/c mice (Figure 1D); fibrosis was more extensive in both strains by day 22 (Figure 1E, F).

Analysis of the livers indicated a highly significant ($p < 0.01$) increase in the amount of protoporphyrin in the livers of the griseofulvin-treated mice closely reflecting the histologic assessment of the protoporphyria (Figure 2B). Both strains of mouse showed a significant elevation of

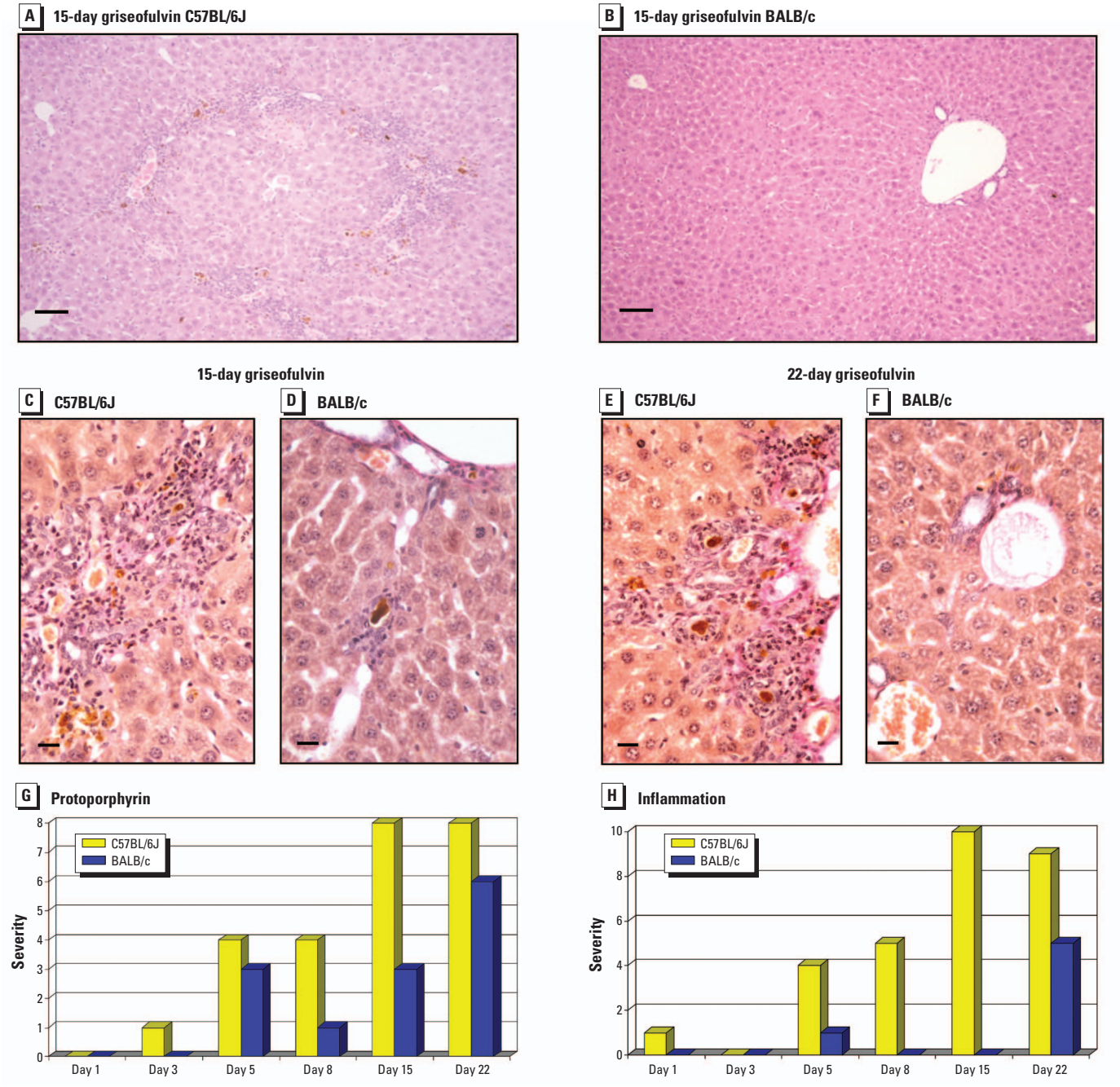

Figure 1. (*A, B*). Low-power views of the liver from 15-day griseofulvin-treated mice: C57BL/6J (*A*) and BALB/c (*B*). (*C, D*) Higher-power views of livers from 15-day griseofulvin-treated mice: C57BL/6J (*C*) and BALB/c (*D*). (*E, F*) Same as for *C* and *D* except they are taken from 22-day griseofulvin-treated mice. (*C–F*) Counterstained with Van Gieson's stain for collagen deposition. (*G*) Histologic assessment of the degree of protoporphyria in the liver. (*H*) Histologic assessment of the degree of inflammation in the livers. A four-point scale was used to assess severity where 0 represented no lesion, 1 = minimal, 2 = moderate and 3 = severe. The scores were totaled for each group of four mice to provide an overall estimate of the severity of these changes. Bars indicate 100 µm on *A* and *B* and 20 µm on *C–F*.

protoporphyrin from day 3, but C57BL/6J mice reached maximal accumulation by day 15 compared with the BALB/c mice, which reached the same level of accumulation by day 22. Plasma ALT and AST levels were markedly elevated from day 3 in both mouse stains and continued to increase significantly relative to controls throughout the study (Figure 2C, D); the increases were greater in the C57BL/6J mice than in the BALB/c strain. AP was elevated from day 5 in the C57BL/6J mice and from day 8 in the BALB/c strain (Figure 2E). The plasma AP levels reflected the marked strain difference in degree of cholestasis.

Having confirmed the development of liver injury and established a strain difference in susceptibility to griseofulvin, the gene expression profiles were analyzed and compared with the pathologic observations and clinical chemistry. The gene expression ratios located in the 95% confidence tail for each microarray were used for clustering analysis (hierarchical using complete linkage) (Figure 3). However, genes were only considered as differentially regulated if the *p* value from four independent experimental ratios was <0.05 compared with the normalized population mean using a two-tailed *t*-test. The original data can be downloaded from the MRC Toxicogenomics Unit website.

Genes associated with pathologic change. Pathologic change was more apparent in C57BL/6J mice than in BALB/c mice (Figure 1), particularly at the later time points, and this correlated with a set of altered gene expressions that are shown in Figure 3A. These genes were associated by gene expression profile, and the overall gene expression profile associated with the degree of pathologic change. Thus, the majority of the genes in this cluster were increased in expression from day 8 in the C57BL/6J mice but not in the BALB/c mice. Functionally, some of these genes are related by association with the initiation and progression of inflammation, and with fibrosis resulting from the tissue repair processes.

Griseofulvin-regulated genes. Altered expression was observed of many genes associated directly with griseofulvin exposure, and these are shown in Figure 3B, D. The genes of these clusters were identified as being differentially expressed as a direct result of griseofulvin exposure rather than subsequent pathologic change in the liver by two further observations. First, there was no association of expression profile of these genes with pathologic change, and second, by comparison with the gene expression profile of a mutant mouse model of ferrochelatase insufficiency (Tutois et al. 1991). In these mice, differential expression (by comparison with wild type) of the genes shown in these clusters (Figure 3B, D) was not observed (unpublished data).

Prominent among these are *Cyp* genes including *Cyp2a4* and *Por* (NADPH cytochrome P450 reductase). The increased expression of *Cyp2a4* observed here may be a cross hybridiation with *Cyp2a5* known to be increased in expression during the development of liver injury and hepatocarcinomas (Camus-Randon et al. 1996; Knasmuller et al. 1997; Salonpaa et al. 1995; Wastl et al. 1998) and is also induced directly by porphyrinogenic agents (Salonpaa et al. 1995). The most highly upregulated *Cyp* genes in this set, *Cyp2b9*, *Cyp2b10*, and *Cyp2b13*, were increased in expression up to 100-fold. Two non-*Cyp* genes reached similar levels of expression. These were the *ALAS 1* that is regulated by heme levels and was responding to decreased heme synthesis and *Gadd45,* a DNA damage-inducible gene.

As members of the same gene superfamily, there is a possibility of cross-reactivity between the *Cyp* genes on the microarray. This was investigated by comparing the sequence homology. Each *Cyp* gene present on the microarray used here was compared with each of the others (unpublished data). The only close homology for the *Cyp* genes regulated in this study is between *Cyp2b10* and *Cyp2b13* where there is an 83% homology based on comparison of the full-length cDNA with no gaps. In Figure 3B these two genes show very similar profiles of differential expression, and it is possible that here we were not measuring the differential expression of both these genes but rather of only one.

Genes increased similarly in expression in both mice strains. Figure 3C shows genes related by expression profile with an increase in expression from days 5 or 8 of the time course in both strains of mice. The gene functions of this cluster are diverse containing among others, *Ly6d* (lymphocyte antigen 6 complex), a lymphocytic marker; *Cstb* (cathespin), an intracellular thiol inhibitor; *Nqo1* (DT-diaphorase) a two-electron quinone oxidoreductase whose expression is often associated with redox stress; and another member of the *annexin* family, others of which are in the cluster shown in Figure 3A; and *Krt8* (Keratin 8), commonly associated with Mallory body formation.

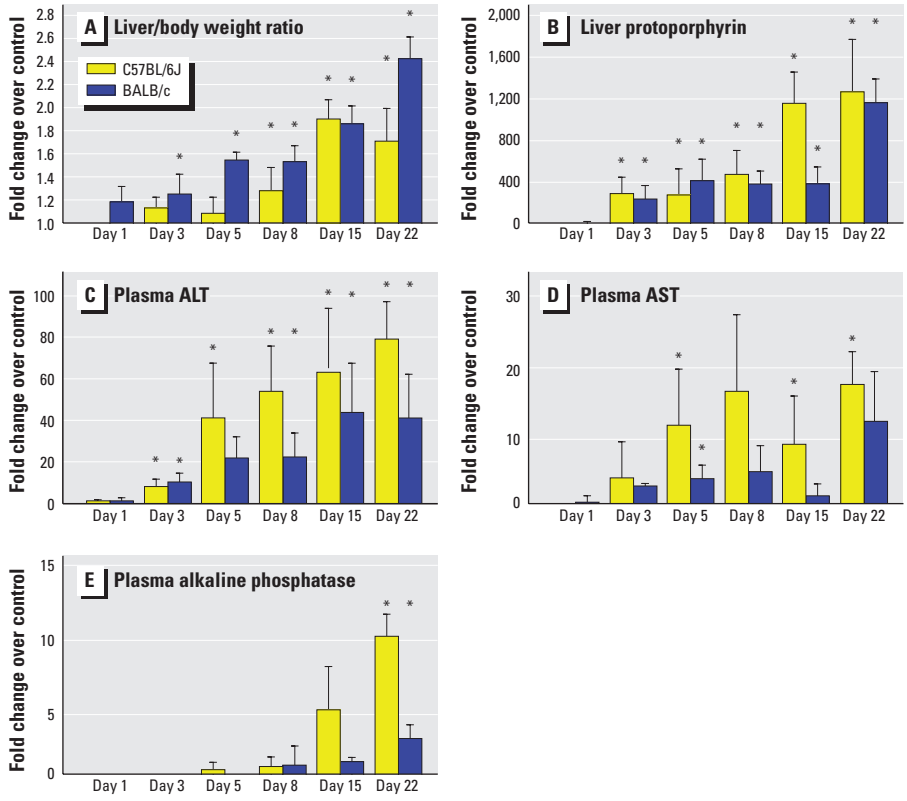

Figure 2. Data are shown as a ratio of the control value (mean control value ± SD for the experiment). (*A*) Liver/body weight ratios (5.13 ± 0.43); (*B*) liver protoporphyrin (0.82 ± 0.39 nmol/g liver); (*C*) plasma ALT (35.2 ± 32.4 U/L); (*D*) plasma AST (83.8 ± 73.06U/L); and (*E*) plasma AP (135 ± 61 U/L). The group size in each case was four mice. Asterisk (*) indicates significant ($p < 0.05$) changes from control. Significance was assessed using a two-tailed paired t-test.

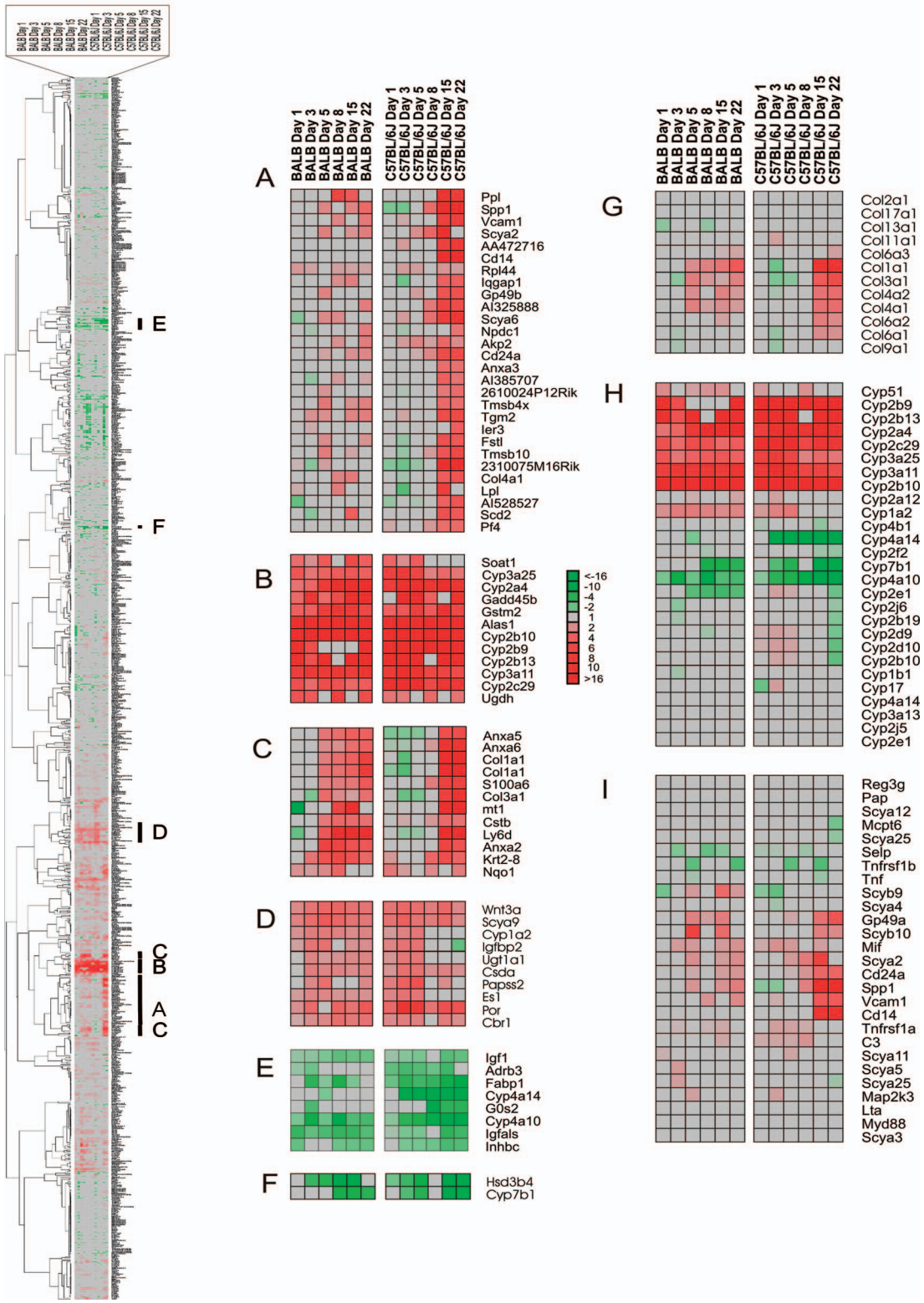

Figure 3. Left panel shows the full gene expression cluster analysis with increased gene expression represented by red and decreased gene expression by green, as indicated by the key. The cluster associated with the BALB/c mice is shown on the left and that for the C57B6/AJ mice on the right with the time course, according to the scale above. (*A*–*F*) Six individual clusters of gene associated by similarity in gene expression profile and the positions of each cluster in the full cluster profile are indicated by the corresponding letter. (*G*–*I*) Sets of genes have been extracted from the main set by family (*G* and *H*) or potential relationship to inflammation (*I*) before being hierarchically clustered. In all cases the genes shown as differentially expressed were significant ($p < 0.05$) by comparison with the normalized population mean using a two-tailed t-test and the mean and SD from four pairs of animals. This resulted in some apparent gaps in responsiveness of individual genes at mid time points compared with adjacent data points, through the time course. This is usually caused by a high variation at these time points and loss of significance. In these cases, therefore, the genes are represented as nondifferentially expressed to maintain the statistical purity of the data, although the trend indicates that the genes are in fact differentially expressed, as would be expected from the time points at either side.

Genes decreased in expression. Genes associated by a similar profile of decreased expression in the griseofulvin-treated mice of both strains are shown in Figure 3E, F. Among this set, Fabp1 (fatty acid–binding protein), also known as a heme-binding protein (Epstein et al. 1994), was decreased in expression, a phenomenon that has been reported previously in griseofulvin-treated liver (Vincent et al. 1989). A downregulated expression of three *Cyp* genes (*Cyp4a10, Cyp4a14,* and *Cyp7b1*) was observed. These are all genes represented by high abundance mRNA, determined from the intensity of the fluorescence on the microarray (unpublished data). *Hsd3b4* (hydroxysteroid dehydrogenase-4, delta^5-3-beta), a critical enzyme in steroid hormone metabolism, was also decreased in expression throughout the time course (Figure 3F).

Clustering by family and function. The clusters in Figure 3A–F were derived through a hierarchical clustering of the genes according to their expression profile. That is, genes that displayed similar expression profiles throughout the time course of both experiments in this study were clustered together regardless of the function of the genes. This is therefore a purely mathematic analysis of the data, and determination of any functional relationship between the genes that are grouped together relies on further analysis. An alternative approach is to cluster the genes according to function or name regardless of their expression profile. This is a much less exacting method of analysis mainly because the functions of many genes are not precisely defined. However, this method of analysis was employed to derive the clusters shown in Figure 3G–I. In Figure 3G all members of the collagen gene family present on the microarrays used have been brought together and then hierarchically clustered. This cluster demonstrates clearly that not all classes of the collagen genes were increased in expression in response to the liver damage. There was also variation within the classes, with two members of the *Col6a* class (1 and 2) being overexpressed but not *Col6a3*. Figure 3H is a cluster of all the family genes present on the microarray. As with the collagen genes, these were first gathered together and then hierarchically clustered. There is a clear distinction between those genes that were decreased in expression versus those that were increased or unchanged.

The final cluster (Figure 3I) is a cluster gathered not by gene family but by function. To examine the response of all genes that might be related to inflammation and therefore altered in expression in response to the changing pathology, the Gene Ontology terms were searched to gather a set of genes that may be related to inflammation. These were then hierarchically clustered. The set of genes overexpressed in the later time points of the C57BL/6J strain shown in Figure 3A can be seen clearly in the middle of the cluster. For the other genes in this set, there was no alteration in expression in either mouse type over the time course of griseofulvin exposure.

Discussion

Our objective in this study was to explore profiles of altered gene expression indicative of ongoing pathology change in the liver. As such, this study forms part of a wider objective to elucidate the relevance and application of genomics to pathologic assessment in both a quantitative and qualitative manner.

Two strains of mice were used in the expectation there would be a difference in response between the strains in a manner similar to that found in human EP where only a subset of individuals develop liver damage. This was confirmed by the presence of a more intense and earlier occurring inflammatory response and associated fibrosis in the C57BL/6J strain compared with that seen in the BALB/c, although the precise reason for these differences was not elucidated. Many of the observed alterations of gene expression were similar between strains with the exception of one large gene cluster (Figure 3A). The different profiles of altered gene expression in the cluster could be directly related through the time course of griseofulvin exposure to changes in pathology and clinical chemistry (Figures 1, 2). Many of the genes in this cluster had a functional association with the processes of inflammation and fibrosis including *a*) *cd14*, a monocyte marker and receptor controlling the release of inflammatory cytokines; *b*) *Scya* (small inducible cytokine subfamily) genes that are monocyte chemotactic proteins; and *c*) *Gp49b*, a leukocyte immunoglobulin-like receptor.

Collagen deposition in and around the biliary tracts could also be correlated with a gene cluster that included increased expression of collagen *1a1, 3a1, 4a1,* and *4a2* genes (Figure 3A, C, G). Of these, *Col1a1* and *Col3a1* often are both involved in wound repair and fibrosis, and associated with cirrhosis in the liver (Harada et al. 1999). Genes associated with wound repair are expressed in fibroblasts in response to serum, including the *Col3a1* gene, and clusters of these genes have also been identified using microarray technology (Iyer et al. 1999). Also overexpressed, though not differentially between the mouse strains, was the *Krt8* (Keratin 8) gene (Figure 3C). Expression of this gene is associated with Mallory body formation, which is known to occur in this model (Denk et al. 1975), and has been observed previously after 1–3 days of feeding griseofulvin at 2.5% of the diet (Cadrin et al. 2000). Additionally, *Krt8* mutations causing keratin accumulation predisposes to liver disease in humans, and its presence here is probably both an indicator of liver disease and a causative factor in the progression of the fibrosis (Ku et al. 2001). Increased *Ly6d* gene expression that was apparent in both mouse strains (Figure 3C) may be related to the lymphocyte infiltration. *Ly6d* is used as a marker for lymphocytes in addition to hemopoietic stem cells and lymphoid precursors (Classon 2001). Its presence here is then probably related to the white cell infiltration. However, there was less inflammation and lymphocyte infiltration apparent in the BALB/c mice compared with the C57BL/6J strain and yet there was a similar increase in expression of the *Ly6d* in both mouse strains. Therefore, either *Ly6d* is an extremely sensitive marker of lymphocyte infiltration or there is another explanation not apparent at the present time. Possibly related to the onset of fibrosis was increased expression of calcyclin (S100a6) (Figure 3C) a calcium-binding protein that is associated with metastasis and with the activation of hepatic stellate cells involved in the development of fibrosis and cirrhosis (Komatsu et al. 2000). The other calcium-binding proteins in this cluster, annexin A2 (*Anxa2*) and annexin A6 (*Anxa6*), are not reported to have such a relationship to fibrosis, but as calcium-binding proteins, and it is interesting to observe that they are increased in expression in the same manner as calcyclin.

Members of the *Cyp* family of genes split into two separate clusters, some were downregulated (Figure 3E, H) and others were very markedly upregulated (Figure 3B, H). Those downregulated were *Cyp4a10, Cyp4a14,* and *Cyp7b1*. *Cyp7b1* is the hydroxylase involved in taurocholate bile acid synthesis in mice (Russell 1999). Unlike *Cyp7a1* this gene does not appear to be downregulated by cholic acid through the farnesoid X bile acid receptor (Sinal et al. 2000). This suggests that regulation of this gene may be occurring through another mechanism sensitive to accumulation of protoporphyrin. Also downregulated was *Hsd3b4,* an enzyme essential in steroid metabolism. Two other *Cyp* genes were downregulated, *Cyp4a10* and *Cyp4a14*. A similar effect on the expression of these *Cyp* genes is seen after treatment with the bacterial endotoxin lipopolysaccharide, which also causes hepatic

inflammation (Barclay et al. 1999). These data suggest that these particular *Cyp* genes may therefore be very sensitive indicators of a liver suffering toxicity. The expression of *Cyp2a5* (coumarin-7-hydroxylase) was induced in both C57BL/6J and BALB/c mice (Figure 3B) and has been associated with development of the neoplastic process (Wastl et al. 1998). This was accompanied by a very marked increase in expression of *Gadd45b* (Figure 3B), a gene associated with DNA damage, which has been previously associated with griseofulvin exposure (Knasmuller et al. 1997).

Increased expression was seen of *Cyp2b10, Cyp2b13, Cyp2c29,* and *Cyp3a11* (Figure 3B). Previous association of griseofulvin with the induction of the *CypP450* genes suggests the induction of these genes here was caused by a direct effect of the griseofulvin rather than by the pathologic change in the liver. This was confirmed by comparison of the data shown here with the gene expression profile of a mouse with homozygous mutation of the ferrrochelatase gene (Tutois et al. 1991). In this mouse there was no induction of the *CypP450* genes shown in Figure 3B (unpublished data). These data confirm that the induction of these *CypP450* genes was a result of a direct effect of griseofulvin and/or its metabolites rather than a consequence of pathologic change. The opposite was true, however, for the downregulated *CypP450* genes in Figure 3E that were also downregulated in the homozygous ferrrochelatase mutant mouse.

To conclude, we have shown that gene expression profiles could be directly related to the evolution of the inflammatory process and subsequent hepatic fibrosis, as well as profiles related to the compound itself and adaptive changes in cellular biochemistry. We have shown the utility and potential ability of gene expression profiles to delineate and predict pathologic change. However, more information is required to model the networks of gene regulation that determine the occurrence and extent of hepatic fibrosis in response to liver damage and inflammation.

References

Barclay TB, Peters JM, Sewer MB, Ferrari L, Gonzalez FJ, Morgan ET. 1999. Modulation of cytochrome P-450 gene expression in endotoxemic mice is tissue specific and peroxisome proliferator-activated receptor-dependent. J Pharmacol Exp Ther 290:1250–1257.

Bellingham RM, Gibbs AH, De Matteis F, Lian LY, Roberts GC. 1995. Determination of the structure of an *N*-substituted protoporphyrin isolated from the livers of griseofulvin-fed mice. Biochem J 307:505–512.

Bissell MD, Gores GJ, Laskin DL, Hoofnagle JH. 2001. Drug-induced liver injury: mechanisms and test systems. Hepatology 33:1009–1013.

Bloomer J, Bruzzone C, Zhu L, Scarlett Y, Magness S, Brenner D. 1998. Molecular defects in ferrochelatase in patients with protoporphyria requiring liver transplantation. J Clin Invest 102:107–114.

Cadrin M, Hovington N, McFarlane-Anderson N. 2000. Early perturbations in keratin and actin gene expression and fibrillar organisation in griseofulvin-fed mouse liver. J Hepatol 33:199–207.

Camus-Randon A-M, Raffalli F, Bereziat J-C, McGregor D, Konstandi M, Lang MA. 1996. Liver injury and expression of cytochromes P450: evidence that regulation of CYP2A5 is different from that of other major xenobiotic metabolizing CYP enzymes. Toxicol Appl Pharm 138:140–148.

Classon BJ. 2001. Ly-6 ligands remain elusive. Trends Immunol 22:126.

Cox TM, Alexander GJM, Sarkany RPE. 1998. Protoporphyria. Semin Liver Dis 18:85–93.

De Matteis F, Rimington C. 1963. Disturbance of porphyrin metabolism caused by griseofulvin in mice. Br J Dermatol 75:91–104.

De Matteis F, Donnelly AJ, Runge WJ. 1966. The effect of prolonged administration of griseofulvin in mice with reference to sex differences. Cancer Res 26:721–726.

Denk H, Gschnait F, Wolff K. 1975. Hepatocellular hyalin (Mallory bodies) in long term griseofulvin-treated mice: a new experimental model for the study of hyalin formation. Lab Invest 32:773–777.

Eisen MB, Spellman PT, Brown PO, Botstein D. 1998. Cluster analysis and display of genome-wide expression patterns. Proc Natl Acad Sci U S A 95:14863–14868.

Epstein LF, Bass NM, Iwahara S-I, Wilton DC. 1994. Immunological identity of rat liver cytosolic heme-binding protein with purified and recombinant liver fatty acid binding protein by Western blots of two-dimensional gels. Biochem Biophys Res Commun 204:163–168.

Friedman SL. 1993. Seminars in medicine of the Beth Israel Hospital, Boston. The cellular basis of hepatic fibrosis. Mechanisms and treatment strategies. N Engl J Med 328:1825–1835.

Gant TW. 2002. Classifying toxicity and pathology by gene-expression profile—taking a lead from studies in neoplasia. Trends Pharmacol Sci 23:388–393.

Grandchamp B, Deybach JC, Grelier M, deVerneuil H, Nordmann Y. 1980. Studies of porphyrin synthesis in fibroblasts of patients with congenital erythropoietic porphyria and one patient with homozygous coproporphyria. Biochem Biophys Acta 629:577.

Hamadeh HK, Bushel PR, Jayadev S, DiSorbo O, Bennett L, Tennant R, et al. 2002a. Prediction of compound signature using high density gene expression profiling. Toxicol Sci 67:232–240.

Hamadeh HK, Bushel PR, Jayadev S, Martin K, DiSorbo O, Sieber S, et al. 2002b. Gene expression analysis reveals chemical-specific profiles. Toxicol Sci 67:219–231.

Hamadeh HK, Knight BL, Haugen AC, Sieber S, Amin RP, Bushel PR, et al. 2002c. Mathapyrilene toxicity: anchorage of pathologic observations to gene expression alterations. Toxicol Pathol 30:470–482.

Harada T, Enomoto A, Boorman GA, Maronpot RR. 1999. Liver and gallbladder. In: Pathology of the Mouse (Maronpot RR, Boorman GA, Gaul BW, eds). Vienna:Cache River Press, 119–183.

Iyer V, Eisen MB, Ross DT, Schuler G, Moore T, Lee JC, et al. 1999. The transcriptional program in the reponse of human fibrobalsts to serum. Science 283:83–87.

Kappas A, Sassa S, Galbraith RA, Nordmann Y. 1995. The porphyrias. In: The Metabolic and Molecular Basis of Inherited Disease (Scriver CR, Benaudet AL, Sly WS, Valle D, eds). New York:McGraw-Hill, 2103–2159.

Knasmuller S, Parzefall W, Helma C, Kassie F, Ecker S, Schulte-Hermann R. 1997. Toxic effects of griseofulvin: disease models, mechanisms and risk assessment. CRC Crit Rev Toxicol 27:495–537.

Komatsu K, Kobune-Fujiwara Y, Andoh A, Ishiguro S, Hunai H, Suzuki N, et al. 2000. Increased expression of S100A6 at the invading fronts of the primary lesion and liver metastasis in patients with colorectal adenocarcinoma. Br J Cancer 83:769–774.

Ku NO, Gish R, Wright TL, Omary MB. 2001. Keratin 8 mutations in patients with cryptogenic liver disease. N Engl J Med 344:1580–1587.

Lee WM. 1995. Drug-induced hepatotoxicity. N Engl J Med 333:1118–1137.

Russell DW. 1999. Nuclear orphan receptors control cholesterol catabolism. Cell 97:539–542.

Salonpaa P, Krause K, Pelkonen O, Raunio H. 1995. Up-regulation of CYP2A5 expression by porphyrinogenic agents in mouse liver. Naunyn-Schmiedebergs Arch Pharmacol 351:446–452.

Shackelford C, Long G, Wolf J, Okerberg C, Herbert R. 2002. Qualitative and quantitative analysis of nonneoplastic lesions in toxicology studies. Toxicol Pathol 30:470–482.

Sinal CJ, Tohkin M, Miyata M, Ward JM, Lambert G, Gonzalez FJ. 2000. Targeted disruption of the nuclear receptor FXR/BAR impairs bile acid and lipid homeostasis. Cell 102:731–744.

Thomas RS, Rank DR, Penn SG, Zastrow GM, Hayes KR, Pande K, et al. 2001. Identification of toxicologically predictive gene sets using cDNA microarrays. Mol Pharmacol 60:1189–1194.

Tilg H, Diehl AM. 2000. Cytokines in alcoholoic and nonalcoholic steatohepatitis. N Engl J Med 343:1467–1476.

Turton NJ, Judah DJ, Riley J, Davies R, Lipson D, Styles JA, et al. 2001. Gene expression and amplification in breast carcinoma cells with intrinsic and acquired doxorubicin resistance. Oncogene 20:1300–1306.

Tutois S, Montagutelli X, Da Silva V, Jouault H, Rouyer-Fessard P, Leroy-Viard K, et al. 1991. Erythropoietic protoporphyria in the house mouse. J Clin Invest 88:1730–1736.

Vincent SH, Smith AG, Muller-Eberhard U. 1989. Modulation of hepatic heme-binding Z protein in mice by the porphyrogenic carcinogens griseofulvin and hexachlorobenzene. Cancer Lett 45:109–114.

Waring JF, Ciurlionis R, Jolly RA, Heindel M, Ulrich RG. 2001. Microarray analysis of hepatotoxins in vitro reveals a correlation between gene expression profiles and mechanisms of toxicity. Toxicol Lett 120:359–368.

Wastl UM, Rossmanith W, Lang MA, Camus-Randon AM, Grasl-Kraupp B, Bursch W, et al. 1998. Expression of cytochrome P450 2A5 in preneoplastic and neoplastic mouse liver lesions. Mol Carcinogen 22:229–234.

Weston Hurst E, Paget GE. 1963. Protoporphyrin, cirrhosis and hepatoma in the livers of mice given griseofulvin. Br J Dermatol 75:105–112.